IUE CAMERA SENSITIVITIES AND THE ECHELLE RIPPLE CORRECTION

Abstract

A study of sensitivity changes with time has been performed for the LWR and SWP cameras by using high dispersion observations of η UMa. Non-uniform changes in response across the camera target are suggested to cause distortions of the observed echelle blaze function for the LWR at high order numbers. Such effects are not seen in the SWP due to its greater stability. Grating constants useful for correction of the echelle ripple are presented. For the SWP, these should be valid for all images taken since 1978. For the LWR, the values are appropriate only for images processed with the new extraction software placed in production in November 1981 (Bohlin and Turnrose 1982).

Introduction

As part of the program to monitor the photometric performance of the IUE cameras, observations of low and high dispersion standard stars have been made periodically since launch. Of highest priority has been the monitoring of low dispersion sensitivity changes, the most recent analysis of which is presented in this Newsletter (Schiffer 1982b). This study indicates that the SWP experienced a short period of degradation in early 1978 and has been steady since then, while the LWR apparently started to change in late 1980 and continues to do so. For both cameras the changes have been non-uniform, that is, different parts of the spectra show different response changes, but in low dispersion it is not possible to tell if the changes are wavelength dependent or are dependent upon the location of wavelengths on the target. Wavelength dependent changes would be evidence, for instance, of radiation damage, while position dependent changes would indicate variations in target gain.

High dispersion observations offer the opportunity to distinguish between wavelength and location dependent changes since each echelle order stretches across the whole target and can be considered roughly constant in wavelength for sensitivity purposes. Unfortunately high dispersion standard star observations in the past have been made less frequently than for low dispersion and until recently were made through the small aperture in order to study any degradation in spectral resolution. Moreover prior to November 1981 the high dispersion extraction processing was considered inadequate for sensitivity monitoring purposes.

Any changes in camera response have several photometric consequences. At the least they affect the absolute flux scale. In low dispersion differential changes will also affect the derived shape of the energy distribution of an object. In high dispersion non-uniformities add further complications because the apparent shape of the echelle blaze function will become distorted. Not only will the absolute energy distributions be affected, but line profiles as well. In fact it has been known for some time that the LWR grating K values, i.e., the wavelength of the observed blaze peak, have been changing with time.

This note is the first report of a camera sensitivity study based on high dispersion observations. It is suggested that changes seen in the LWR are not wavelength dependent, but rather are a function of position on the camera target. Thus the observed shape of the echelle ripple changes with time, increasing the difficulty of deriving reliable correction parameters. Too few observations are available for the SWP during its early period of change to derive conclusions about wavelength/location dependency, but its greater stability allows a unique set of blaze function parameters to be determined.

Sensitivity Study

Only one standard star, η UMa, has been observed often enough to provide suitable coverage for sensitivity monitoring. Because observations through the small aperture result in variable throughput, only large aperture exposures can be used. This reduces the number of useable images to 15 for the LWR and 16 for the SWP (table I). All the images were reprocessed with the new extraction software to provide a homogeneous set of data.

For each camera, an image taken in late 1979 was selected as a baseline image against which others would be compared. The other spectra were resampled to the baseline wavelength scale, smoothed by a 5-point box car filter, ratioed with the smoothed baseline fluxes, and binned. Exposure times were corrected for camera response time (Schiffer 1980), but were not corrected for sensitivity changes with temperature (Schiffer 1982a) so that an examination could be made for differential temperature effects across the camera target. Thus the effective exposure time is

$$t_{eff} = \text{integer}(t_{obs}/0.4096) \times 0.4096 - .12 \text{ secs.}$$

Two analyses were performed for each camera. To study gross changes, average ratios were calculated in 9 regions centered on orders m = 82, 97, and 112 at the nominal central wavelength ($\lambda_c = K/m$, K = 231150 for LWR and 137725 for SWP) and the half-power points along each order. Secondly a more detailed analysis was made by sampling 31 points along 31 nearly equally spaced orders. Figure 1 illustrates the areas sampled for each case.

The LWR shows a strong non-uniform change in sensitivity, with greater degradation along the long-wavelength part of each order and towards higher orders. Figure 2 demonstrates the changes seen in two regions of little and large variation. In low dispersion there is evidence that the camera response was nearly constant until late 1980 when a period of decrease began. Too few high dispersion spectra are available to confirm the early stability, but in some areas the later observations show large scale changes. To quantify the differential changes, we have determined linear rates of change with time (which probably underestimate recent changes) in table II. Also shown are the values for the SWP, which are found to be much smaller and more uniform across the camera.

For these regressions, temperature variations (as measured by the camera head amplifier temperature thermistor, THDA) were also solved individually for each region as well as forcing one temperature dependence for all areas. When examined by region, the mean uncertainty in the temperature coefficients, $\pm$0.41 %, was larger than the scatter in the coefficients themselves, $\pm$0.21 %.

From the limited data available then, a single temperature correction can be applied to the whole image; we find for the LWR, -1.0 ± 0.2 % /°C (THDA-12), for the SWP -1.1 ± 0.1 %/°C (THDA-8). These values compare favorably with those found by Schiffer for low dispersion.

For the fine analysis, images were temperature corrected and linear rates were computed for each of the 31 x 31 regions. To decrease the noise, these points were smoothed by a 3-point triangular filter and are presented as contour plots in figure 3. The median rate of change for the LWR is -1.8 ± 0.7 % per year, for the SWP -0.7 ± 0.7 % per year. The contours are plotted at levels of $\pm 2n\sigma$ from the median. They graphically illustrate the rate of degradation in the upper left of the LWR.

Sensitivity Effects on the Observed Blaze Function

The effect of differential changes across the LWR to the observed blaze function can be seen in figure 4a. The decrease in sensitivity at the long-wavelength end of the order causes an apparent shift of the blaze peak towards shorter wavelengths, makes the blaze function appear narrower, and decreases the net flux. This becomes evident when attempting to optimize the blaze correction parameters, as described by Ake (1981). Assuming a blaze function of the form

$$\mathrm{sinc}^2 \, m\pi\alpha \, (1-K/m/\lambda) \ ,$$

least-squares fits are performed to optimize the K and α values. The K values are found to be order dependent while α is relatively constant. Figure 4b illustrates the LWR K values derived for an early and recent image compared with the mean of all images. For orders greater than about $m = 95$, the K values have been decreasing in time, reflecting the shift towards shorter wavelengths of the observed peaks. When the spectra are examined as they were originally processed, these problems are found to have been accentuated by the old extraction software.

Echelle Blaze Function Parameters

With these caveats in mind, it appears that a unique set of K and α parameters can be determined for all SWP images taken since 1978, but those for the LWR, particularly for orders greater than 95, will have to be updated from time to time. Because of the changes seen in the LWR, sensitivity monitoring observations are being obtained more frequently now.

Figure 5a illustrates the mean SWP K values for the images listed in table III. The majority of the spectra are those of η UMa, but to minify the dependence of the observed blaze with spectral type (more because of spectral lines than temperature differences), other objects were added. Except for the η UMa images, the spectra were reduced with the processing in use at the time of observation. The variation of K with order can be fit by a quadratic of the form

$$K_{SWP} = 138827 - 27.426 \ m + 0.165883 \ m^2$$

and the optimum value for α is 0.856 ± 0.03.

For the LWR it is possible to derive a mean relation only for the most recent observations. Table III lists those images obtained since the new extraction processing was introduced. Figure 5b illustrates the mean variation of K for these, and a quadratic fit to the data yields

$$K_{LWR} = 230036 + 15.3456\ m - 0.050638\ m^2$$

where K is appropriate for wavelengths converted to air values, as those for IUE are for $\lambda \geq 2000$ A. The optimum value for α is 0.896 ± 0.03. K values for older images can be approximated by this relation for orders less than m = 95.

Observers wishing to correct their own data with these values will have to be aware that the wavelengths given in the new extraction are heliocentric while the ripple correction should be made in the rest frame of the spacecraft. The velocity values applied to any particular image are listed in the processing header.

References

Ake, T. B. 1981, NASA IUE Newsletter, 15, p. 60

Bohlin, R. and Turnrose, B. 1982, NASA IUE Newsletter, 18, p. 29

Schiffer, F. H. 1980, NASA IUE Newsletter, 11, p 33.

1982a, NASA IUE Newsletter, 18, p. 64

1982b, this Newsletter.

Thomas B. Ake

8 July 1982

Table I: LARGE APERTURE OBSERVATIONS OF ETA UMA

Date (Year/Day)	LWR Image Number	LWR Exp Time	LWR THDA	SWP Image Number	SWP Exp Time	SWP THDA
			°C			°C
1978/245	2245	6 sec	11.2	2249	6 sec	6.5
1979/013	3480	7	12.5	3910	7	7.5
159	4733	4	12.2	5456	4	5.1
197	5069	5	13.8	5820	5	8.8
252	5541*	7	11.5	6458*	7	6.8
1980/048	6948	7	13.8	7974	6	9.1
202	8303	6	12.5	9549	6	5.8
282	8969	6	12.8	10306	6	8.2
294	9111	9	13.5	10429	10	7.8
307	9210	6	14.5	10522	6	10.8
361	9580	6	14.2	10894	6	9.5
1981/068	10102	6	17.2	13439	6	14.5
218	11258	6	10.8	14673	6	7.5
264	-	-	-	15068	6	4.8
313	11948	6	14.2	15458	6	9.5
1982/009	12319	6	14.2	16002	6	8.5

*
Baseline images for comparison

Table II: GROSS SENSITIVITY VARIATIONS (% Change per Year)

Area	LWR	SWP
1	-1.43	-1.34
2	-1.31	-0.65
3	-1.73	-0.27
4	-1.60	-0.74
5	-2.81 ± 0.71	-0.73 ± 0.59
6	-3.61	+0.19
7	-2.42	+0.24
8	-2.42	-0.10
9	-5.59	+1.06
THDA	-1.04 ± 0.17	-1.08 ± 0.09 (% per °C)

Table III IMAGES USED FOR DETERMINING MEAN K VALUES

Image Number	Object	Spec Type	Image Number	Object	Spec Type
LWR 12319	Eta UMa*	B3 V	LWR 12975*	+28 4211	O4 VI
12484	Tau Sco*	B0 V	12978*	Eta UMa	B3 V
12537	Zet Cas*	B2 IV	13028*	Lam Lep	B0 IV
12616	Tau Sco*	B0 V	13121*	Eta UMa	B3 V
12617	Tau Sco*	B0 V	13247*	Eta UMa	B3 V
SWP 1537	Mu Col	O9 V	SWP 11127	+28 4211	O4 VI
1542	+28 4211	O4 VI	11128	Lam Lep	B0 IV
5778	+28 4211	O4 VI	13439*	Eta UMa	B3 V
5779	+28 4211	O4 VI	13541	G191-B2B	DA wk
6458*	Eta UMa	B3 V	16002*	Eta UMa	B3 V
8683	Tau Sco	B0 V	16714*	Eta UMa	B3 V
9551	+75 325	O5 VI	16877*	Eta UMa	B3 V
10306*	Eta UMa	B3 V	16962*	Eta UMa	B3 V
10522	Eta UMa	B3 V			

* Processed with new extraction software

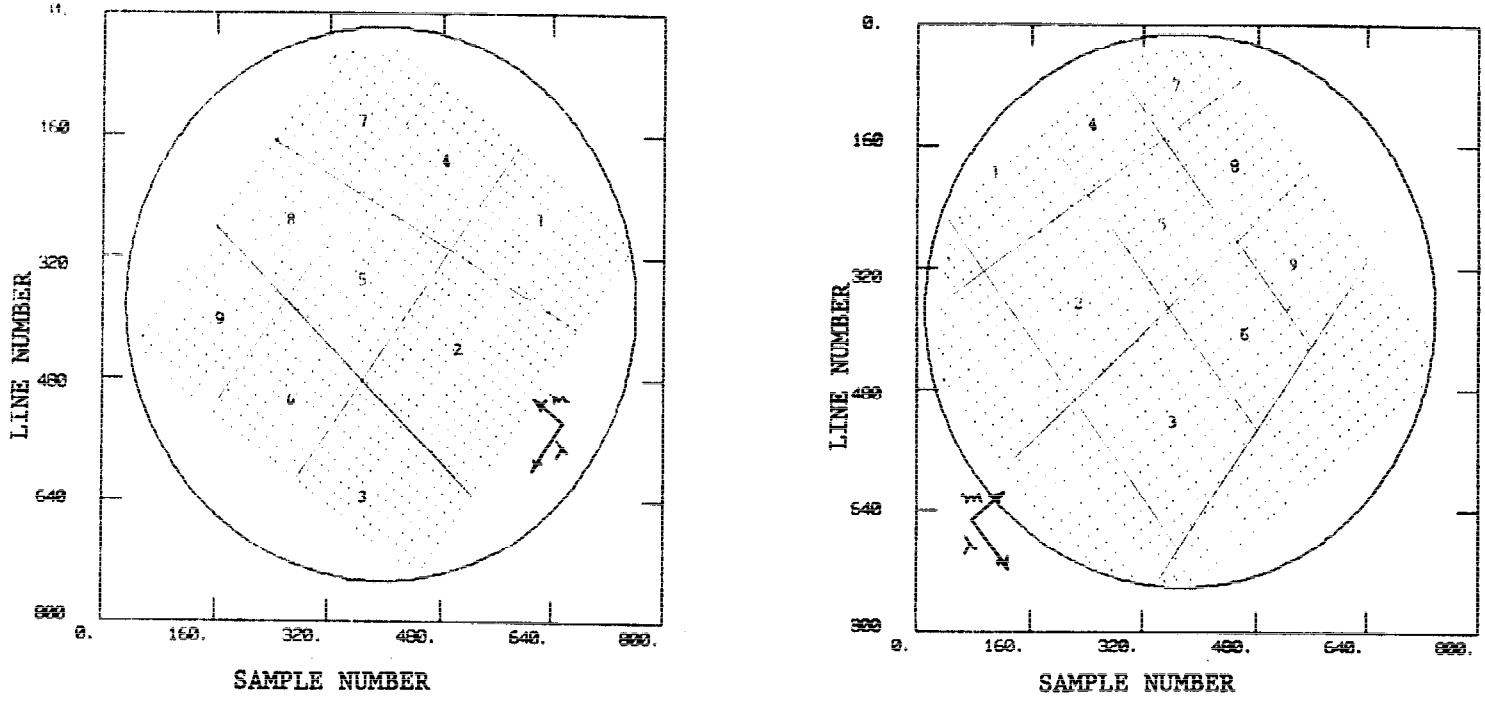

Figure 1. Areas sampled for LWR (left) and SWP (right) sensitivity variations. Boundaries are shown for gross analysis, dots for fine analysis. Arrows indicate direction of increasing order number and wavelength along an order.

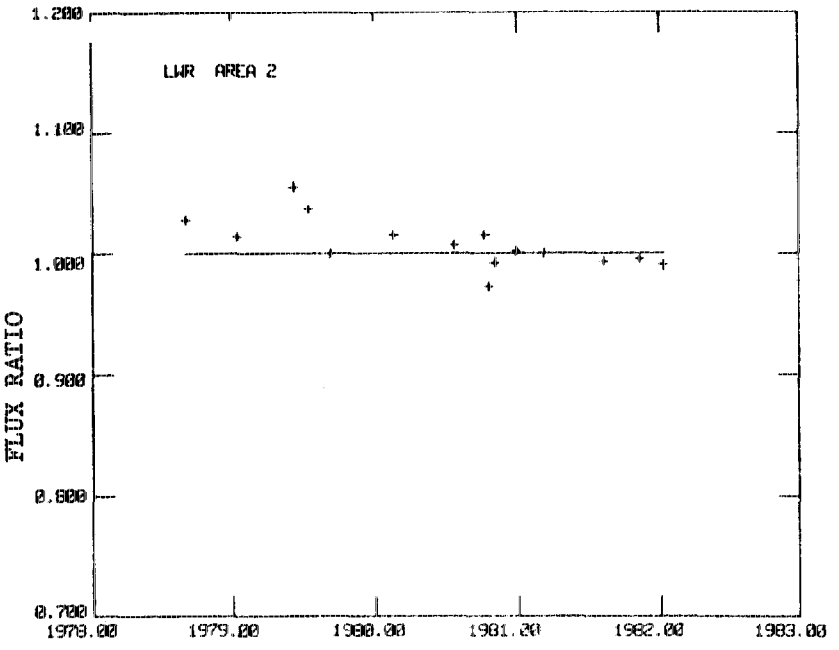

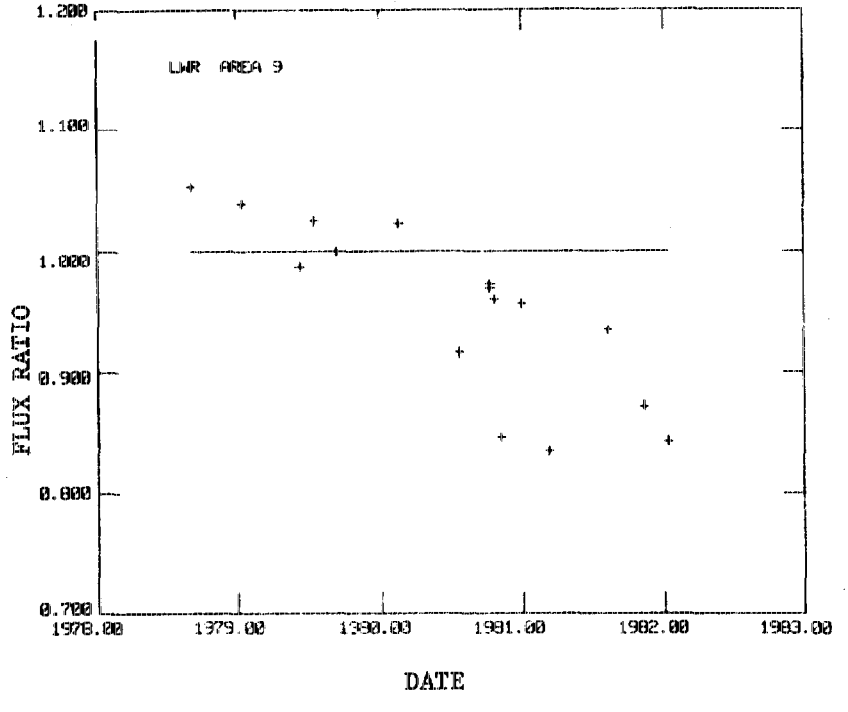

Figure 2. LWR sensitivity changes in two gross regions.

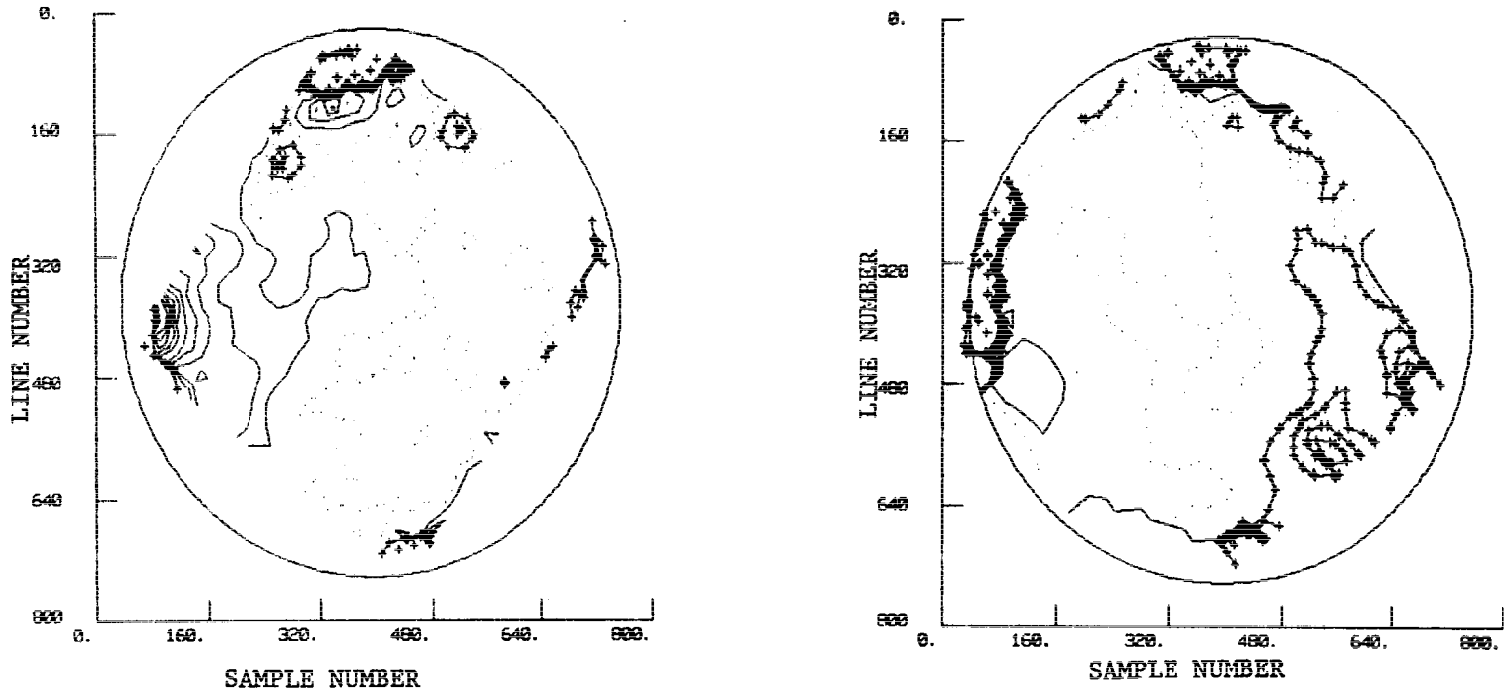

Figure 3. Contour plots of LWR (left) and SWP (right) sensitivity rates with time. Dots are levels through the median values -1.8 %/yr for LWR, -0.7 %/yr for SWP. Other levels are spaced at $\pm$ 2nσ levels, n = 1...10, σ = 0.7%/yr. Pluses indicate areas of median + 2nσ, lines are median -2nσ.

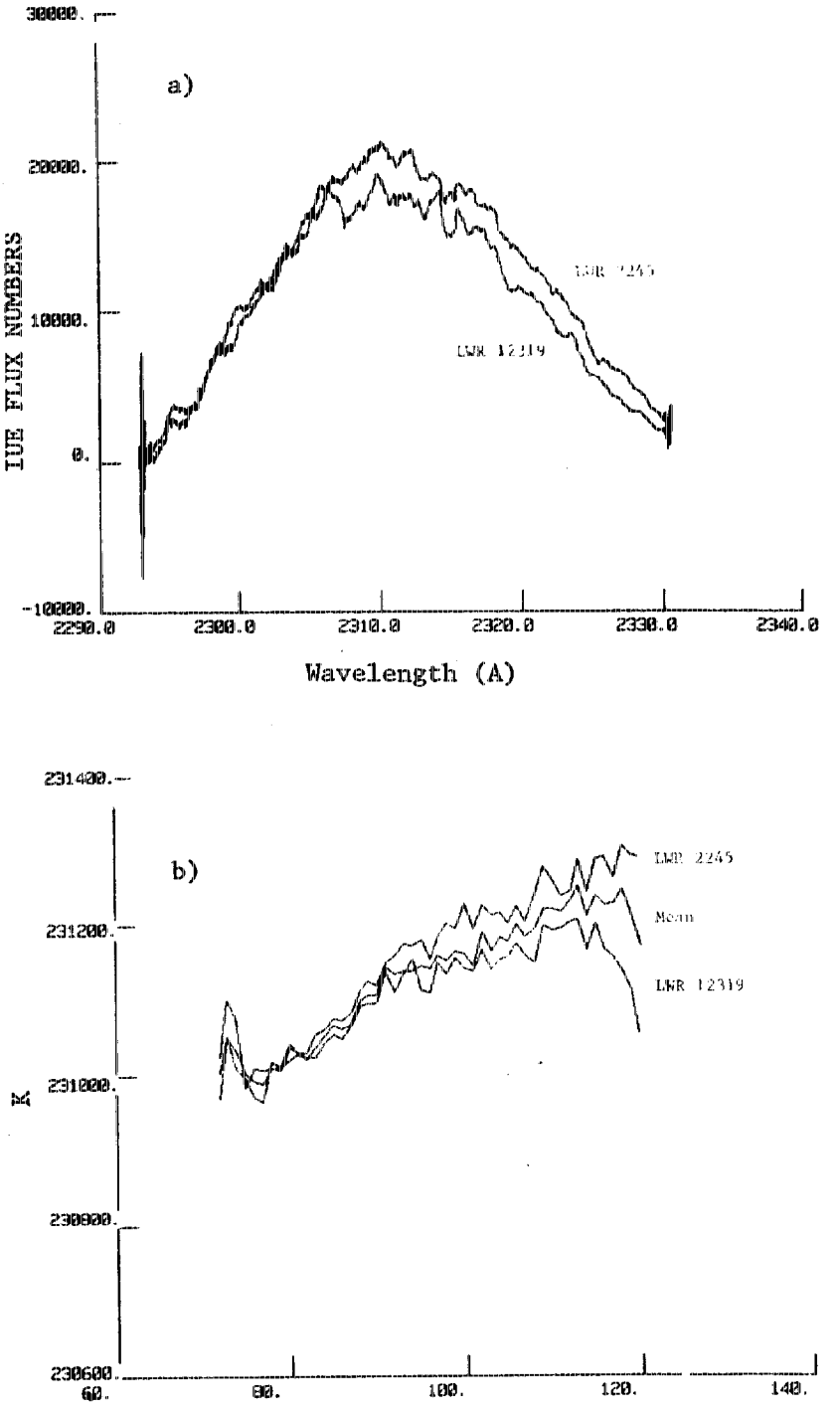

Figure 4. a). Net spectra of an early and a recent LWR exposure of η UMa.

b). K values for these images. The mean line is for all η UMa images.

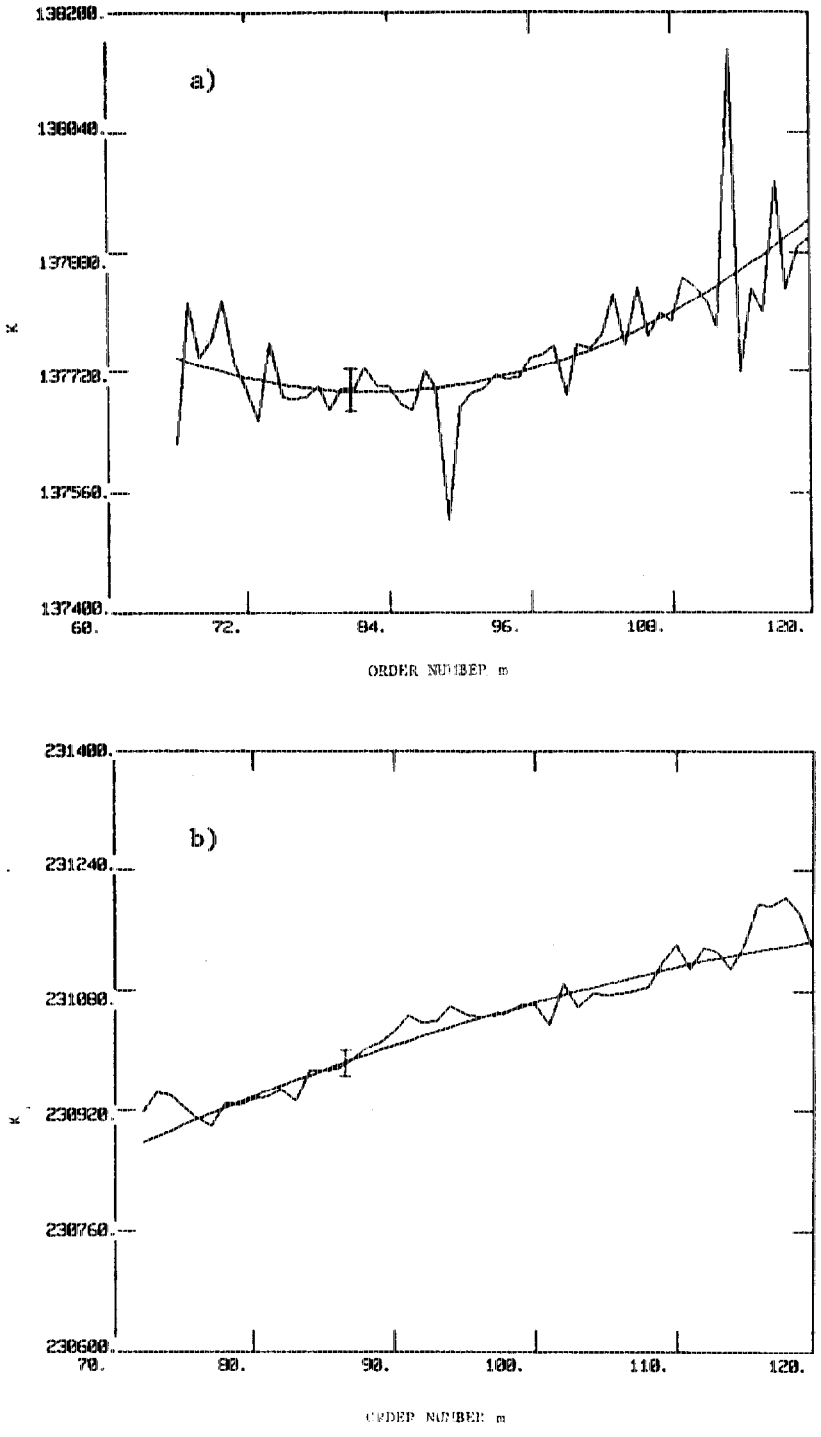

Figure 5. a) SWP mean K variation with order for images in table III. Shown is the quadratic fit and mean error bar.

b) Same as above for LWR.